Engineered Science

RESEARCH PAPER View Article Online

Fabrication of Thermally Stable Graphite-Based Poly(acrylonitrile-co-acrylic acid) Composite with Impressive Antimicrobial Properties

Nasrullah Shah,[1*] Sobia Aslam,[1] Mazhar Ul-Islam,[2] Muhammad Balal Arain,[3] Touseef Rehan,[4] Muhammad Naeem,[1] Muhammad Wajid Ullah[1*] and Guang Yang[5*]

The current study reports the synthesis of graphite-based poly(acrylonitrile-co-acrylic acid) composite (GPC) sheets *via* sol-gel/casting method. The effect of different amounts of graphite (0.25 to 40 wt%) on various characteristics of the prepared GPC was studied through scanning electron microscopy (SEM), Fourier transform infrared spectroscopy (FTIR), X-ray diffraction analysis (XRD), and differential thermal gravimetric analysis (TGA/DTG). The XRD and FTIR analyses confirmed the existence of characteristic peaks of graphite while SEM micrographs showed its uniform distribution in polymer matrix. TGA curves revealed enhancement of thermal stability of GPC with increasing graphite content. The swelling ratio and water holding capacity analyses revealed a reduced hydrophilic behavior of GPC with increasing graphite content. The fabricated GPC demonstrated impressive antimicrobial properties against *Escherichia coli*. The structural, physico-chemical, thermal, and biological features of as-prepared GPC show their potential biomedical applications.

Keywords: Poly(acrylonitrile-co-acrylic acid); Graphite; Composites; Thermal properties; Antimicrobial activity

Received 6 January 2019**, Accepted** 9 February 2019

DOI: 10.30919/es8d758

1. Introduction

The polymers-based composites are receiving immense consideration with growing research owing to their improved and novel features as compared to pure polymers themselves.[1] Various features of pure polymers including conducting,[2–4]thermal,[5] biocompatible,[6,7] and antimicrobial,[8,9] etc. have been improved through impregnation of nanoparticles or blending with other biocompatible polymers.[10] Polymers are less expensive and possess high strength-to-weight ratios and can be easily processed to acquire specific shapes. However, low thermal conductivities and diffusivity, low thermal stability, high electrical resistivity, and ductile mechanical properties make the polymeric material relatively less applicable in various fields.[11] Besides, most of the pure polymers have weak biological features including biocompatibility, degradability and antimicrobial activities which hinder their broad-spectrum applications in biomedical and other fields.[5,12–15]

The intrinsic properties of polymeric materials can be improved by synthesizing their composites.[16–19] The polymers-based composites are the synthetic materials which are made of polymeric matrix and filler. The fillers or additives improve the existing properties of polymer composites and enable them to be used for different applications. The polymer-based composites have been prepared with a verity of organic and inorganic additive materials including nanoparticles, nanofibers, and polymers, etc.[16,20] by using different techniques such as *in situ* addition, *ex situ* impregnation, polymer blending, and sol-gel casting, etc.[10,13,14,21]. The use of carbon-based nanofillers is of great interest in the field of nanocomposites. Graphite is favorable in this regard due to its low price, easy availability, abundance, and several potential applications.[22,23] The polymeric materials containing graphite have been widely explored for their electrical conductivity and stability. Graphite has been used in the fabrication of composite materials for coating,[24] bipolar plates,[25] grid,[26] electrode,[27–29] electrochemical, and biosensors.[30–32]

A recent study reported the preparation of polycarbonatediol polyurethane composites with different amounts of graphite conductive filler and studied the effect of graphite contents on the molecular motions and conductivity phenomenon of the polymeric materials.[33] In another study, Mironov *et al.* studied the electrical conductance properties of graphite-based powdery polypropylene and polyvinylidene fluoride (PVDF) composites.[34] Akin *et al.* incorporated different amounts of carbon fiber and expanded the graphite to synthesize cyclic olefin copolymer composites. They reported an enhancement in the electrical conductivity of the composites.[35] The PVDF/graphite composites prepared by the solution precipitation method clearly indicated that varied concentration of graphite significantly affected the crystallization behavior of the composite and improved its dielectric constant as compared to pure PVDF.[36] Park*et al* reported the synthesis of polymer/reduced graphite oxide (rGO) composite nanoparticles. They emulsified AMPS-modified rGO in the presence of styrene and butyl acrylate monomer that on further polymerization produced poly(St-co-BA)/rGO

[1]*Department of Chemistry, Abdul Wali Khan University Mardan, Mardan, Pakistan*
[2]*Department of Chemical Engineering, College of Engineering, Dhofar University, Salalah,Sultanate of Oman*
[3]*Department of Chemistry, University of Karachi, Karachi, Pakistan*
[4]*Department of Biochemistry, Quaid-i-Azam University, Islamabad, Pakistan*
[5]*Department of Biomedical Engineering, Huazhong University of Science and Technology, Wuhan 430074, P. R. China*
***E-mail:** nasrullah@awkum.edu.pk; wajid_kundi@hust.edu.cn; yang_sunny@yahoo.com*

composite latex nanoparticles. The as-synthesized composites demonstrated high electrical conductivity.[37] Natural-flake graphite/polymer (NFG/polymer) composite sheets were prepared by Zhou *et al via* tape-casting method. They evaluated the in-plane thermal conductivities of the composites and found that graphene incorporation provided better thermal conductivity than CNTs.[38] The polymer composites have also been synthesized for augmenting the bactericidal and biocompatible features of pure polymers.[9,39–47] Besides, these have been applied for fabricating scaffold materials.[48–52] Such composites find potential applications in devising medical devices.

The current study is aimed to synthesize a biocompatible and biodegradable composite comprised of poly(acrylonitrile-co-acrylic acid) matrix with graphite as an additive in different proportions. The as-synthesized graphite-based composite showed improved structural characteristics, thermal stability, and antimicrobial activity, thus can find potential biomedical applications, such as in scaffold development and packaging materials where all these properties are required.

2. Experimental section

2.1 Chemicals and materials

The acrylic acid (AA) and acrylonitrile (AN) were obtained from Yakuri Pure Chemicals Co., (Osaka, Japan). The 2,2-azobisisobutyronitrile (AIBN) was obtained from Junsei Chemical Co., Ltd. (Japan) and dimethylsulfoxide (DMSO) was the product of Duksun Pure Chemical Co., (Korea). Similarly, trifluoroacetic acid (TFA) and graphite powder were purchased from Sigma-Aldrich (St Louis, MO, USA). Distilled water was used in all experiments. All reagents used were of analytical grade and were used without further processing.

2.2 Preparation of PAN-co-AA

Poly(acrylonitrile-co-acrylic acid) (PAN-*co*-AA) was synthesized by our previously reported method.[53] Briefly, for preparation of PAN-*co*-AA, 7.51 g of AA was added to 50.43 g of DMSO and 2 mL of TFA followed by the addition of 37.72 mL of AN and 0.22 g of AIBN dissolved in 50 g of DMSO. The final solution was stirred and purged with N_2 gas and copolymerization was carried out under N_2 atmosphere for 6 h at 200 rpm and 60 °C. Finally, 100.86 g of DMSO was added into thick viscous polymer solution and stirred for about 20 h at 200 rpm and 25 °C.

2.3 Preparation of graphite-based PAN-co-AA composites

For synthesis of graphite-based PAN-co-AA composite, 1.0 g of graphite powder was weighed and added to PAN-co-AA solution. For uniform dispersion of powder inside the polymer matrix at a controlled temperature, physico-mechanical techniques were employed. First, the suspension was vortexed for 15 min at 2,000 rpm. Following vortexing, the mixture was sonicated for 15 min at 45 °C to fully disperse the graphite within the polymer matrix and air bubbles were removed from the suspension. The mixture was converted to sheet by casting *via* sol-gel method. For this purpose, a washed and completely dried glass slab was placed on a smooth surface. The solution was poured over it. A glass rod was used to spread the solution on the slab in a rolling manner. The slab was placed in a tub of distilled water. The synthesized composites sheets dipped in distilled water were washed and preserved for future use. Following the above procedure, different graphite-based PAN-co-AA composites were prepared by adding different wt% of graphite (0.25%, 5%, 20%, 30%, and 40%) into PAN-*co*-AA solution. A 10 mL of PAN-*co*-AA solution was used as a control. The copolymer solution was converted to sheet by casting and sol-gel method. The synthesized sheets dipped in distilled water were washed and preserved for future use.

2.4 Characterization of graphite-based PAN-co-AA composites

The synthesized composites were characterized for various features by using different analytical tools. Scanning electron microscopy (SEM) of the freeze-dried control and GPC sheets was performed using a Hitachi S-4800 & EDX-350 (Horiba) FE-SEM (Tokyo Japan). Rectangular strips cut from copolymer PAN-co-AA and graphite-based composite sheets were fixed on the brass holder and coated with OsO_4 by VD HPC-ISW osmium coater (Tokyo Japan) prior to SEM observation. The SEM micrographs of the surface and cross section were taken. For FTIR analysis, all synthesized copolymer PAN-*co*-AA and various GPC sheets were dried by mild heating and freeze-drying. Initially, the sheets were kept in a pre-heated oven at 110°C for 30 min. Finally, all samples were refrigerated for 1 day and then freeze-dried at -51 °C. After drying, the FTIR spectra were taken by inserting the sample strips one by one directly to the path of incident radiation using a Nicolet S10 FTIR spectrometer (Thermo Scientific, USA) in a range of 400-4000 cm^{-1} with an attenuated total reflectance (ATR) mode. The thermogravimetric analysis (TGA) and differential thermal analysis (DTA) analyses of all freeze-dried samples were conducted on a thermo-balance by heating the samples from room temperature to 1000 °C at 10 °C/min in a N_2 flow. X-ray diffraction spectra of control and GPC were recorded by X'Pert-APD Phillips, Netherlands) with an X-ray generator (3 KW) and anode (LFF Cu). The radiation was Cu Ka with a wavelength of 1.54 Å. The X-ray generator tension and current were 40 kv and 30 mA, respectively. The sheets were cut into small pieces and placed in powder sample stage for analysis.

2.5 Physical tests of graphite-based PAN-co-AA composites

Rectangular strips were prepared from as-synthesized PAN-co-AA copolymer and GPC sheets in order to investigate their physical characteristics including thermal study, percent swelling ratio (%SR), water holding capacity (WHC), and water evaporation rate (WER). The rectangular wet strips were first surface-dried by using soft tissue paper and their weights were measured. The weighed-strips were put on a glass slab and labeled. The glass slab was kept in a pre-heated oven at 110 °C for 30 min. After 30 min, the strips were taken out of the oven and weighed again. All dry strips of control and GPC sheets were put in pan having appropriate amount of distilled water for different time interval and weighed again. The water swelling ratios of control and various GPC sheets was studied by determining their distilled water adsorption capacity at different time intervals from 1 min to 4 days (6,000 min) at room temperature. The percent mass swelling was calculated using the following formula:

$$swelling(\%) = \frac{M_t - M_0}{M_0} \times 100 \quad \text{(A.1)}$$

where M_0 and M_t are the initial weight and weight at different time intervals, respectively.

The water holding capacity (WHC) of control and GPC sheets was calculated using the following formula:

$$WHC = \frac{W_0 - W_m}{W_m} \quad \text{(A.2)}$$

where W_m is the freeze-dried weight (g) of the membrane.

2.6 Antibacterial activity of graphite-based PAN-co-AA composites

Antibacterial activities of all samples were investigated against *E. coli* by both optical density and colony-forming unit (CFU) methods. In

optical density method, the dried samples were sliced into small pieces and sterilized at 121 °C for 15 min. A 10 mL of *E. coli* growth medium was taken in each tube. Next, 1.0 mL *E. coli* culture and 0.01g/mL of finely sliced samples were added to each tube and incubated at 37 °C and 150 rpm for 18 h. During incubation, the turbidity of the medium was observed at 615 nm using a UV spectrophotometer (Jasco V-650). In the CFU method, 0.01 g/mL finely sliced and autoclaved samples were added to *E. coli* growth medium in separate test tubes. Controls were made without samples. The tubes were seeded with 1 mL of fresh *E. coli* culture and incubated at 37 °C and 150 rpm for 12 h. 100 µL of each sample was spread on plates containing *E. coli* agar medium. These plates were incubated at 37 °C for 24 h. Following incubation, colonies were counted and results between plates were compared.

3. Results and discussion

3.1 Effect of temperature on stability of GPC sheets

The digital photographical images of rectangular strips cut from PAN-co-AA copolymer and GPC sheets kept at 110 °C for 1 h period is given in Fig. 1. For all samples, the evaporation of physiosorbed water and volatilization of volatile components from the rectangular strips resulted in a rapid weight loss. However, the composite sheets with increasing graphite content illustrated a lower weight loss. Among all samples, PAN-*co*-AA exhibited a high degree of expansion.[54] In contrast, a dramatic increase in the thermal resistivity was observed from the images with the increased graphite content in virgin PAN-*co*-AA copolymer (Fig. 1). The results showed more distortion in the sheets with high copolymers content and small quantity of graphite. This phenomenon argues that the presence of graphite in polymer matrix enhanced its thermal resistivity. Furthermore, the stability was enhanced distinctly up to 20 wt% graphite contents.

3.2 Structural morphology of PAN-co-AA and GPC

The morphology of the virgin PAN-*co*-AA copolymer and GPC sheets was investigated through SEM analysis. Fig. 2 represents the surface and cross-sectional micrographs of PAN-*co*-AA and various composite films. The top view of PAN-*co*-AA film shown in Fig. 2 (A) reveals a three-dimensional porous structure with small needle-like appearance. The morphology of copolymer was significantly changed with the introduction of graphite and formed a homogeneously distributed film (Figs. 2B, C, and E). Similar morphological variation have been reported by Shan *et al*.[53] This change in morphology is attributed to the interaction between PAN-*co*-AA and graphite. A gradual increase in the

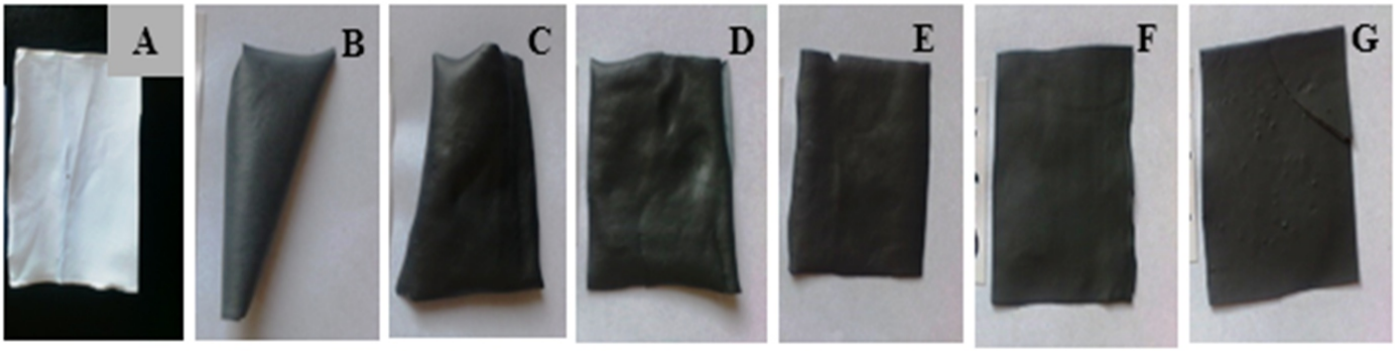

Fig. 1 Photographs showing the effect of temperature on PAN-*co*-AA (control) (A) and GPC sheets with 0.25 wt% (B), 5 wt% (C), 10 wt% (D), 20 wt% (E), 30 wt% (F), and 40 wt% graphite (G), respectively, kept at 110 °C in drying oven for 40 min.

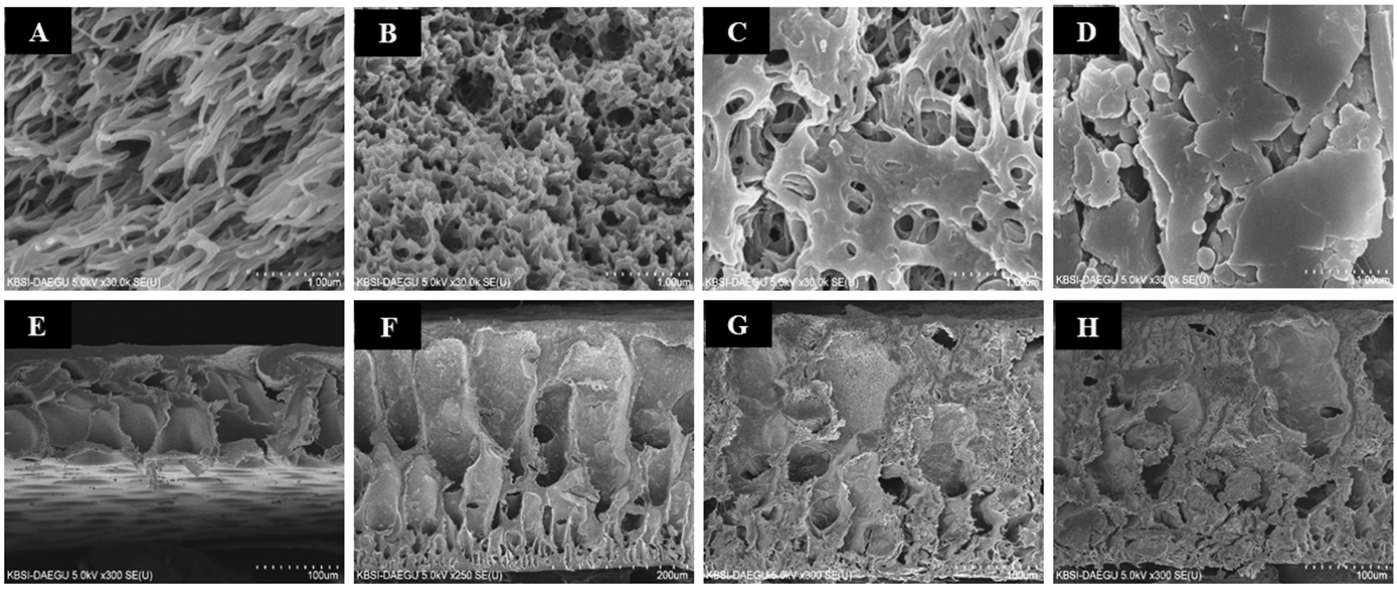

Fig. 2 SEM micrographs of the surface and cross section of PAN-co-AA (A and E) and GPC with different amount of graphite 5wt% (B and F), 20 wt% (C and G) and 40 wt% (D and H).

graphite content into the copolymer matrix finally resulted in the aggregation of copolymer. Hence, the copolymer fused together into a single, continuous sheet as showed in Fig. 2. Further, SEM micrographs showed uniform dispersion of graphite powder into PAN-*co*-AA. Like the surface analysis of virgin PAN-*co*-AA copolymer and GPC sheets, an obvious difference was observed in the cross-sectional morphologies (Figs. 2 (E-H). The results indicated that graphite was successfully incorporated into the three-dimensional porous structure of PAN-*co*-AA. The internal incorporation and formation of homogenous composites would ultimately bless the composites with improved physiological, thermal, and biological features.

3.3 Chemical structure analysis of PAN-co-AA and GPC

The FTIR spectrum of PAN-*co*-AA and GPC is shown in Fig. 3. The characteristic bands corresponding to different functional groups were identified and listed in Table 1. The FTIR spectrum of virgin PAN-*co*-AA copolymer exhibited characteristic bands at 2923, 2243, 1436, and 1719 cm^{-1}, which were assigned to C-H bending, C-N stretching, CH_2 bending for PAN segments, and C-O stretching for AA segments, respectively. Furthermore, the band appeared near 3292 cm^{-1} region was assigned to the OH stretching vibration from free carboxylic acid of the copolymer as reported by Shan *et al.*[55] Few other peaks appeared in the finger print region were attributed to C-C and C-N stretching vibrations. Similar functional groups were observed for GPC sheets. However, a slight change was observed in the range for C=O stretching, CH_2 bending, C-N stretching, and C-C stretching frequency. Some characteristics peaks assigned to various functionalities of control and 5 wt% and 20 wt% added graphite are summarized in Table 1. It is obvious that with the incorporation of 5 wt% and 20 wt% graphite, no new bands were observed. This absence of new peaks in PAN-*co*-AA after graphite insertion might be due to the absence of any additional functional group in the graphite, which is in agreement with a previous report.[56]

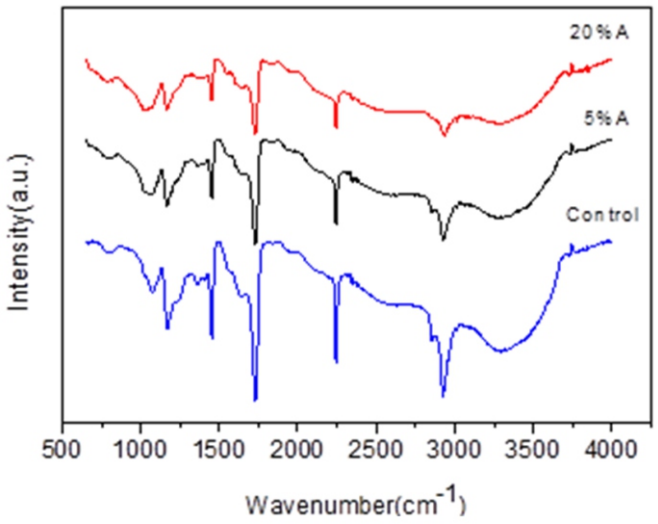

Fig. 3 FTIR spectra of PAN-*co*-AA and 5 wt%, 20 wt% GPC sheets.

3.4 Thermal properties of PAN-co-AA and GPC

The thermal decomposition behavior of PAN-*co*-AA and all analytical grade graphite-based composite sheets prepared in current study are shown in Fig. 4 (A and B). As indicated from Fig. 4A, the first weight loss for all samples was observed around 110 °C, that is most probably attributed to the desorption of small amount of physiosorbed water. The second and major weight loss occurred due to the thermal degradation of PAN-*co*-AA copolymer in the range of 230 °C to 550 °C. This corresponds to the appearance of two DTG peaks; one centered at 281 °C and the other at 506 °C as shown in Fig. 4B, indicating two-step thermal degradation of PAN-*co*-AA copolymer. The first step ranged from 230 °C to 370 °C with maximum speed of degradation at 281 °C while the second one varied from 370 °C to 600 °C with a maximum degradation speed at 506°C. The first exotherm as revealed from DTG analysis corresponds to decomposition of acrylic acid (AA) into anhydride by dehydration of acid group. The anhydride was then decomposed through decarboxylation. At the same time, acrylonitrile (AN) also went through the process of dehydrogenation and stabilization *via* cyclization. However, these thermal transformations were overlaid by the decomposition of AA.

Table 1 FTIR spectra interpretation of PAN-*co*-AA and GPC.

S/No.	Wavenumber (cm^{-1})			Functional group
	Control	5%	20%	
1	3290.12	3292.24	3292.50	OH stretch
2	2923.24	2923.56	2923.12	C-H stretch
3	2243.56	2243.24	2243.3	$C \equiv N$ stretch
4	1719.28	1747.84	1733.56	C=O stretch (for AA)
5	1436.40	1450.68	1450.00	CH_2 bending (forPAN)
6	1167.12	1167.12	1181.40	C-N stretch
7	1053.56	1039.28	1011.40	C-C stretch

In the second step of degradation and appearance of exothermic peak at DTG, the AN went through aromatization and graphitization between 370 °C to 600 °C as reported by Dima *et al.* [57] The TG and DTG curves of 0.25 wt%, 5 wt%, 10 wt%, 20 wt%, 30 wt%, and 40 wt% analytical grade graphite-based composite sheets are also shown in Fig. 4A and Fig. 4B, respectively. As shown in Figs. 4 (A and B), the thermal degradation of the entire composite sheets took place in the temperature range of 230 °C to 550 °C. This range is the same as appeared for PAN-*co*-AA. This might be since graphite is thermally stable up to 600 °C. No change in weight loss was observed from the TG curves of various composite sheets upon the incorporation of graphite which is attributed to the high thermal stability of graphite as reported previously.[56] However, the DTG curves of 30 wt% and 40 wt% composites showed slightly different behavior from other samples. DTG curves indicated that with increasing graphite contents, the second step acrylonitrile decomposition peaks were reduced which is attributed to the extreme graphitization in the presence of large quantity of graphite powder that prevented the thermal degradation of AN. Thus, the excessive amount of graphite provided thermal stability to the composite sheets.

3.5 XRD of PAN-co-AA and GPC

X-ray diffraction patterns of PAN-*co*-AA (control) and 5 wt%, 20 wt%, and 40 wt% GPC sheets are given in Fig. 5. A comparison of 2θ values along with the intensities of XRD peaks for these four samples are also listed in Table 2. PAN-*co*-AA exhibited an intense diffraction peak centered at 2θ of 17.07° indexed as 100 reflection, which is associated with a hexagonal structure of polyacrylonitrile (PAN) similar to that

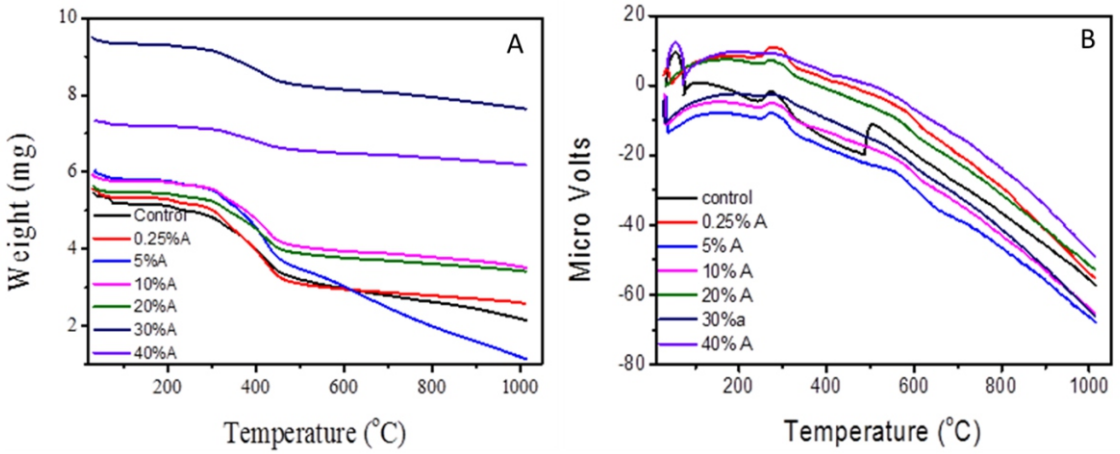

Fig. 4 (A) TG curves of control (PAN-*co*-AA) and GPC sheets and (B) DTG curves of control (PAN-*co*-AA) and GPC sheets.

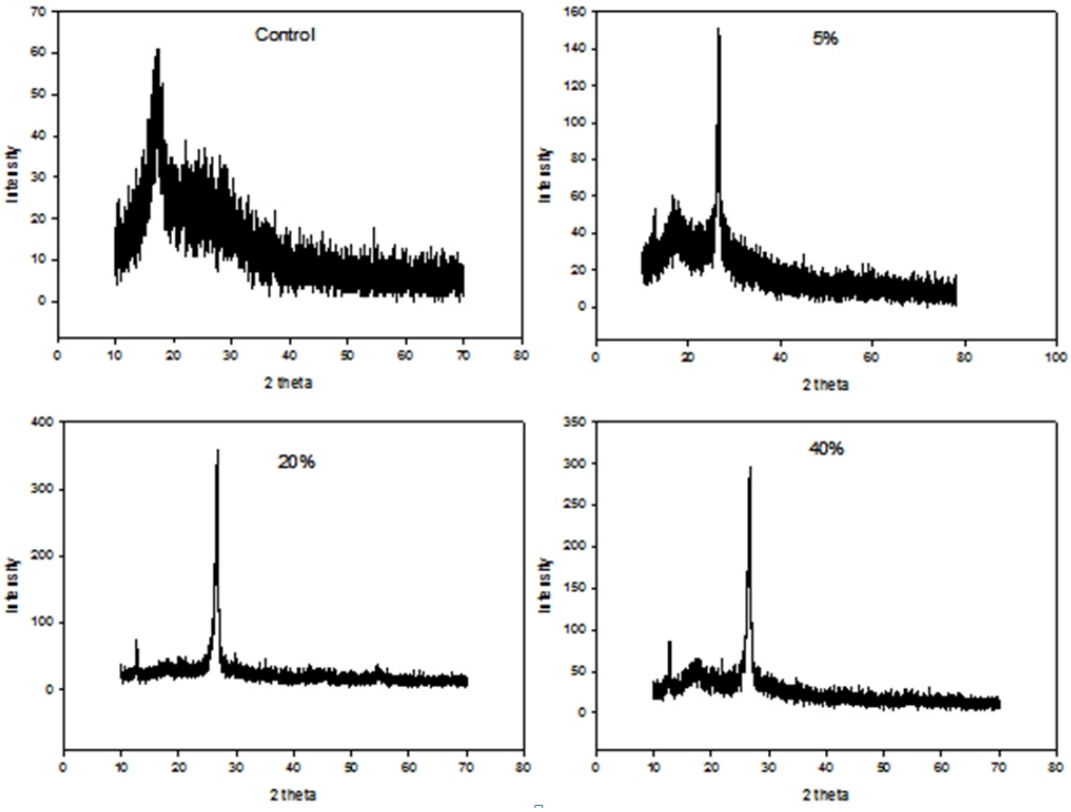

Fig. 5 XRD of control (PAN-*co*-AA) and GPC sheets.

Table 2 Comparison of XRD peaks of PAN-*co*-AA (control) and GPC sheets showing their 2θ values and intensities.

Control	5 wt% GPC	20 wt% GPC	40 wt% GPC
2θ	2θ	2θ	2θ
-	12.62	12.72	12.8
17.07	16.38	17.84	17.11
-	26.60	26.66	26.65

reported by Lee *et al*.[58] XRD pattern for 5 wt%, 20 wt%, and 40 wt% graphite-based composite sheets indicated an additional peak at 2θ value of 26.60° along with the main diffraction peak at 2θ of 17.07°. The appearance of this peak augments the existence of graphite in the structure of PAN-*co*-AA. Similar peak at 2θ of 26.5° indexed as 002 reflection was observed by Naebe *et al* [59] for graphite. The appearance of the peak at 2θ=26.5° ensured a prolonged stabilization of copolymer associated with the 002 planes of graphitic structure due to cyclization and crystallization of co-polymer as reported in literature.[60] Thus, from the above results, it can be concluded that the original structure of PAN-*co*-AA was changed due to stabilization with the incorporation of graphite.

3.6 Swelling behavior and water holding capacity analysis of PAN-co-AA and GPC

The swelling behavior of the composite materials is very important from medical perspective.[61] Fig. 6 shows a comparison of swelling ratios of PAN-*co*-AA (control) with GPC sheets at different time intervals ranging from 1 min up to 4 days (6,000 min) at room temperature. Fig. 7 clearly shows that a maximum swelling was obtained for PAN-*co*-AA (control) as compared to GPC sheets. This is due to the presence of hydrophilic groups such as acrylic acid (AA) and acrylonitrile (AN).[62,63] The incorporation of different quantities of graphite enhanced the hydrophobic sites in the composites which in turn resulted in reduced interaction with water and that consequently led to less water absorption. The ultimate result is a sharp decrease in SR from 0.25 wt% to 40 wt%. Therefore, the incorporation of hydrophilic or hydrophobic groups in the copolymers can control the behavior of phase transition as reported previously.[64] Furthermore, Fig. 6 elucidated the swelling rate which was faster in the first 90 min due to availability of hydrophilic groups and free space. The rate decreased with the passage of time and with the reduction in water binding sites.

The WHC of PAN-*co*-AA (control) and various analytical grade graphite-based composite sheets was obtained after drying their completely swelled wet sheets at room temperature. The WHC results shown in Fig. 7 clearly illustrate that a maximum WHC was achieved for PAN-*co*-AA (control) as compared to the analytical grade composite

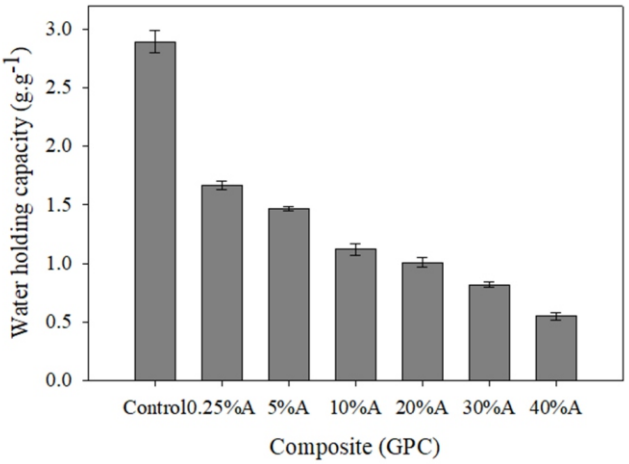

Fig. 7 Water holding capacity of control (PAN-*co*-AA) and GPC sheets.

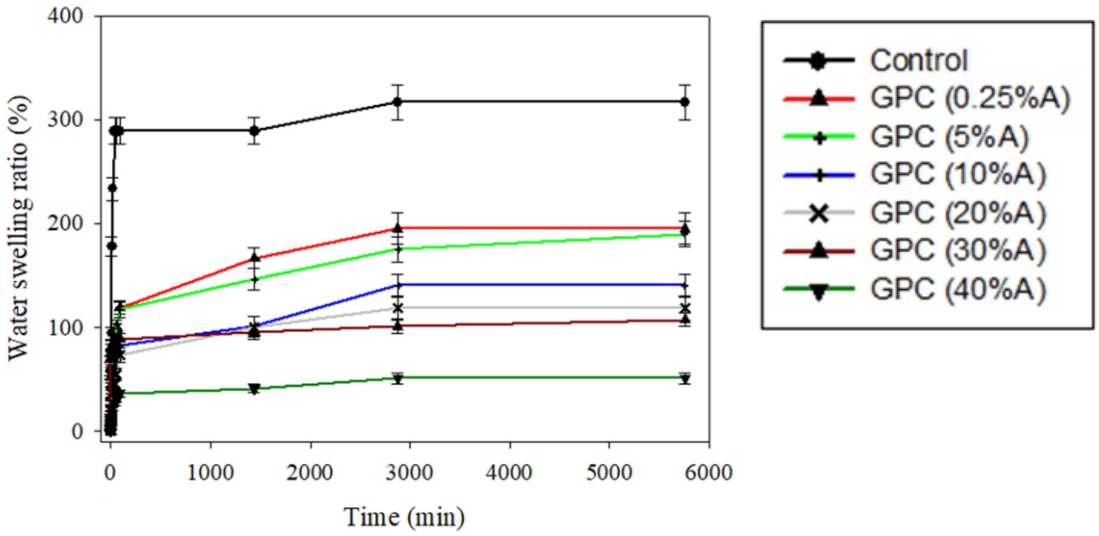

Fig. 6 Swelling ratio of control (PAN-*co*-AA) and GPC sheets.

sheets. This is since both monomers AN and AA in the copolymers are hydrophilic in nature. The absorption capacity increased with the increase in the quantities of both AN and AA. The enhancement of absorption capacity due to the acrylonitrile is reported by Kiatkamjornwong and Faullimmel.[62] The hydrophilic nature of AA is reported by Mahdavinia *et al*.[63] The incorporation of graphite (hydrophobic) reduced the number of hydrophilic groups of the copolymer which led to the weakening of interaction between water and hydrophilic groups of the copolymer. Consequently, a sharp decrease in WHC was observed in PAN-*co*-AA with the incorporation of increasing graphite contents from 0.25 wt% to 40 wt%.

3.7 Antibacterial activity of PAN-co-AA and GPC

The GPC composite showed high antimicrobial activity against *E. coli* as shown in Table 3. Fig. 8 also shows the colony forming results of control and GPC sheets. The results showed that the incorporation of graphite blessed bactericidal features to the composites and the effect enhanced with the increasing graphite contents. Fig. 8 indicates a visible difference in CFU count even with 5 wt% graphite contents and the effect became more prominent with 20 wt% and 40 wt% GPC composites. Table 3 data also supported the CFU results which indicate around 30% to 40 % reduction in bacterial colonies in 20 wt% and 40 wt% GPC. This indicates that graphite has played a vital role in the cytotoxicity that could be attributed to the physical stress on membrane and oxidative stress on *E. coli* maintained by the graphite additive of each GPC.[65] The incorporation of bactericidal nature in such composites can furnish various applications in medical fields.

4. Conclusions

The current study demonstrated successful fabrications of graphite-based poly(AN-co-AA) composite (GPC) sheets using simple physico-mechanical

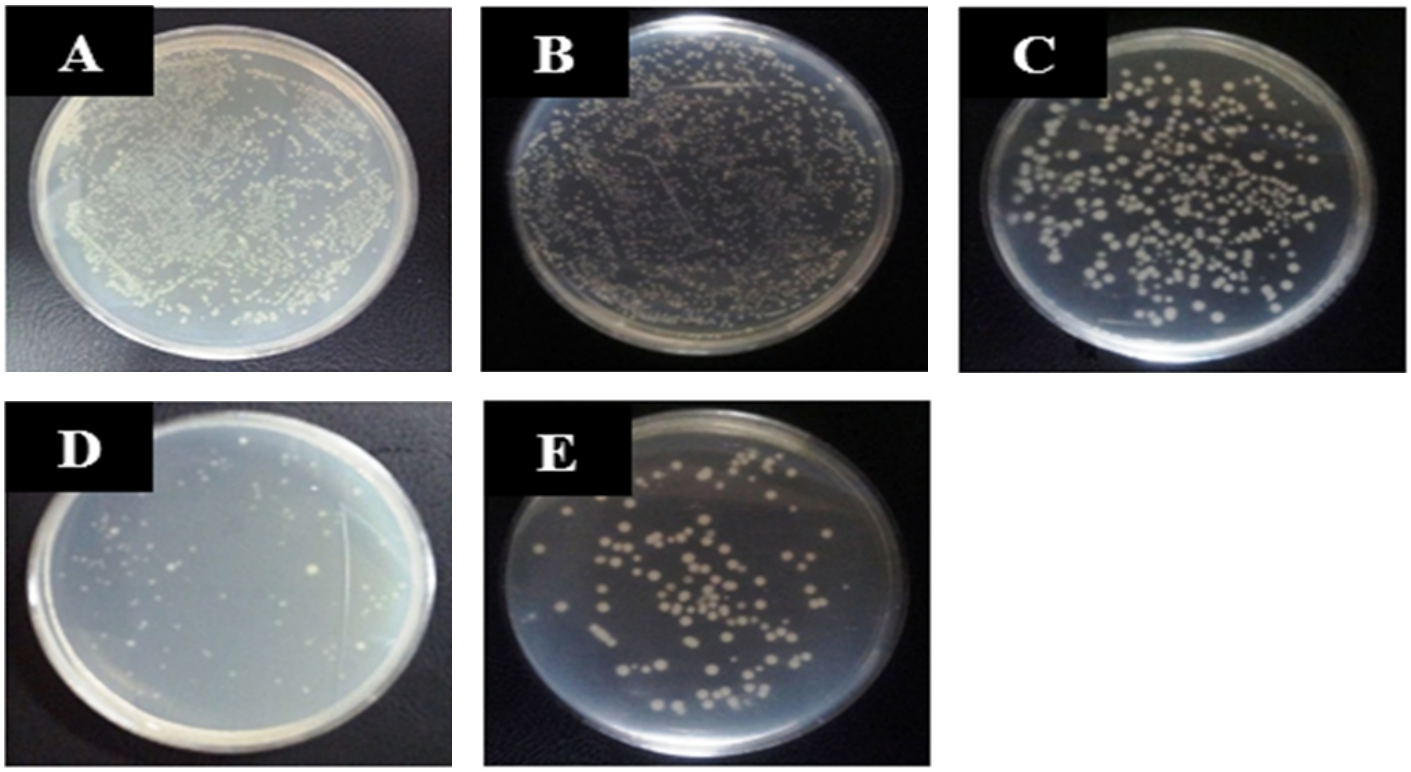

Fig. 8 Antibacterial study of control (only media) (A), control (PAN-*co*-AA) (B) and of GPC 5 wt% (C), 20 wt% (D), and 40 wt% (E).

Table 3 Antimicrobial activity of GBC using *E. Coli* strain at different interval of time.

Time (hr/s)	Control (only media)	Control	5%GPC	20%GPC	40%GPC
0.0	0.02	0.02	0.02	0.02	0.02
3.0	0.31	0.3	0.24	0.21	0.19
6.0	0.53	0.49	0.42	0.36	0.3
12.0	0.72	0.64	0.59	0.50	0.42
18.0	0.93	0.85	0.70	0.62	0.51

technique followed by sol/gel process. Various characterization techniques such as SEM, FTIR, TGA/DTG, and XRD were employed to study the structural features of the resultant GPC sheets. Structural analysis revealed homogenous distribution of graphite inside the composite sheets that resulted in impressive physical and thermal features. The GPC sheets illustrated a boost in higher thermal stability with increasing graphite content. A decrease in hydrophobicity was observed as the amount of graphite was increased in the GPC sheets. Furthermore, the biological tests revealed their impressive antimicrobial properties against *E. coli* that intern augment their multiple applications especially in biomedical fields and conductive devices.

Conflict of interest

There are no conflicts to declare.

Acknowledgements

This research was fully funded by Higher Education Commission (HEC) of Pakistan under NRPU-2014 grants (No. 3868, 3925), National Natural Science Foundation of China (31270150, 51603079, 21774039), China Postdoctoral Science Foundation (2016M602291), and Fundamental Research Funds for Central Universities, Open Research Fund of State Key Laboratory of Polymer Physics and Chemistry, Changchun Institute of Applied Chemistry, Chinese Academy of Sciences.

References

1. M. Ul-Islam, S. Khan, M. W. Ullah and J. K. Park, *Structure, Chemistry and Pharmaceutical Applications of Biodegradable Polymers*, 2015, 517–540.
2. S. Khan, M. Ul-Islam, W. A. Khattak, M. W. Ullah and J. K. Park, *Carbohydr. Polym.*, 2015, **127**, 86–93.
3. A. Jasim, M. W. Ullah, Z. Shi, X. Lin and G. Yang, *Carbohydr. Polym.*, 2017, **163**, 62–69.
4. S. Li, A. Jasim, W. Zhao, L. Fu, M. W. Ullah, Z. Shi and G. Yang, *ES Mater. Manuf.*, 2018, 41–49.
5. M. W. Ullah, M. Ul-Islam, S. Khan, Y. Kim, J. H. Jang and J. K. Park, *RSC Adv.*, 2016, **6**, 22424–22435.
6. L. Lamboni, Y. Li, J. Liu and G. Yang, *Biomacromolecules*, 2016, **17**, 3076–3084.
7. M. U. Islam, S. Khan, W. A. Khattak and J. K. Park, in *Eco-friendly Polymer Nanocomposites*, 2015, pp. 399–337.
8. Z. Shi, X. Gao, M. W. Ullah, S. Li, Q. Wang and G. Yang, *Biomaterials*, 2016, 111, 40–54.
9. M. Ul-Islam, A. Shehzad, S. Khan, W. A. Khattak, M. W. Ullah and J. K. Park, *J. Nanosci. Nanotechnol.*, 2014, **14**, 780–791.
10. N. Shah, M. Ul-Islam, W. A. Khattak and J. K. Park, *Carbohydr. Polym.*, 2013, 98, 1585–1598.
11. I. H. Tavman, A. Turgut, H. M. Da Fonseca, H. R. B. Orlande, R. M. Cotta and M. Magalhaes, *Int. J. Thermophys.*, 2011, **34**, 2297–2306.
12. M. Ul-Islam, S. Khan, M. W. Ullah and J. K. Park, *Biotechnol. J.*, 2015, **10**, 1847–1861.
13. M. Ul-Islam, W. A. Khattak, M. W. Ullah, S. Khan and J. K. Park, *Cellulose*, 2014, **21**, 433–447.
14. S. Khan, M. Ul-Islam, M. W. Ullah, M. Israr, J. H. Jang and J. K. Park, *Int. J. Biol. Macromol.*, 2018, **107**, 865–873.
15. Z. Di, Z. Shi, M. W. Ullah, S. Li and G. Yang, *Int. J. Biol. Macromol.*, , DOI:10.1016/j.ijbiomac.2017.07.075.
16. P. Vilímová, J. Tokarský, P. Peikertová, K. Mamulová Kutláková and T. Plaček, *Polym. Test.*, 2016, **52**, 46-53.
17. Y. Zhang, K. Y. Rhee and S. J. Park, *Compos. Part B Eng.*, , DOI:10.1016/j.compositesb.2017.01.051.
18. Y. Zhang, Y. J. Heo, Y. R. Son, I. In, K. H. An, B. J. Kim and S. J. Park, *Carbon N. Y.*, 2019, **142**, 445-460.
19. Y. Zhang, J. R. Choi and S. J. Park, *Compos. Part A Appl. Sci. Manuf.*, , DOI:10.1016/j.compositesa.2018.04.001.
20. R. Pal, M. J. Akhtar and K. K. Kar, *Polym. Test.*, , DOI:10.1016/j.polymertesting.2018.06.011.
21. S. Khan, M. Ul-Islam, M. Ikram, S. U. Islam, M. W. Ullah, M. Israr, J. H. Jang, S. Yoon and J. K. Park, *Int. J. Biol. Macromol.*, 2018, **117**, 1200–1210.
22. Y. Yin, B. Jiang, X. Zhu, L. Meng and Y. Huang, *Eng. Sci.*, 2018, 17–19.
23. S. M. Lebedev, O. S. Gefle, E. T. Amitov, D. Y. Berchuk and D. V. Zhuravlev, *Polym. Test.*, 2017, **58**, 241–248.
24. J. K. Katiyar, S. K. Sinha and A. Kumar, *Wear*, , DOI:10.1016/j.wear.2016.06.011.
25. A. Adloo, M. Sadeghi, M. Masoomi and H. N. Pazhooh, *Renew. Energy*, , DOI:10.1016/j.renene.2016.07.062.
26. S. Zhang, H. Zhang, J. Cheng, W. Zhang, G. Cao, H. Zhao and Y. Yang, *J. Power Sources*, , DOI:10.1016/j.jpowsour.2016.09.097.
27. N. Gedam, N. R. Neti, M. Kormunda, J. Subrt and S. Bakardjieva, *Electrochim. Acta*, , DOI:10.1016/j.electacta.2015.04.058.
28. C. Calixto, R. Mendes and A. Oliveira, *Mater. Res.*, 2007, **10**, 109–114.
29. X. Li, W. Zhao, R. Yin, X. Huang and L. Qian, *Eng. Sci.*, 2018, 89–95.
30. S. Ku, S. Palanisamy and S. M. Chen, *J. Colloid Interface Sci.*, 2013, **8**, 029.
31. C. Rajkumar, B. Thirumalraj, S. M. Chen and H. A. Chen, *J. Colloid Interface Sci.*, 2017, **487**, 149-155.
32. T. H. Seah and M. Pumera, *Sensors Actuators, B Chem.*, 2011, **156**, 79-83.
33. C. M. Gómez, M. Culebras, A. Cantarero, B. Redondo-Foj, P. Ortiz-Serna, M. Carsí and M. J. Sanchis, in *Appl. Surf. Sci.*, 2013, **275**, 295-302.
34. V. S. Mironov, J. K. Kim, M. Park, S. Lim and W. K. Cho, *Polym. Test.*, 2016, **10**, 169-180.
35. D. Akin, A. Kasgoz and A. Durmus, *Compos. Part A Appl. Sci. Manuf.*, DOI:10.1016/j.compositesa.2014.01.008.
36. F. He, J. Fan and S. Lau, *Polym. Test.*, DOI:10.1016/j.polymertesting. 2008.08.010.
37. N. Park, J. Lee, H. Min, Y. D. Park and H. S. Lee, *Polymer (Guildf).*, DOI:10.1016/j.polymer.2014.08.029.
38. S. Zhou, J. Xu, Q. H. Yang, S. Chiang, B. Li, H. Du, C. Xu and F. Kang, *Carbon N. Y.*, , DOI:10.1016/j.carbon.2013.02.018.
39. S. B. K. M. S. Ahmed, T. Kamal, S. A. Khan, Y. Anwar, M.T . Saeed, A.M. Asiri, *Curr. Nanosci.*, 2016, **12**, 569–575.
40. F. Ali, S. B. Khan, T. Kamal, Y. Anwar, K. A. Alamry and A. M. Asiri, *Chemosphere*, DOI:10.1016/j.chemosphere.2017.08.118.
41. F. Ali, S. B. Khan, T. Kamal, Y. Anwar, K. A. Alamry and A. M. Asiri, *Carbohydr. Polym.*, 2017, **173**, 676–689.
42. T. Kamal, N. Ali, A. Naseem, S. Khan and A. Asiri, *Recent Pat. Nanotechnol.*, , DOI:10.2174/1872210510666160429145704.
43. T. Kamal, M. Ul-Islam, S. B. Khan and A. M. Asiri, *Int. J. Biol. Macromol.*, , DOI:10.1016/j.ijbiomac.2015.08.060.
44. S. A. Khan, S. B. Khan, T. Kamal, M. Yasir and A. M. Asiri, *Int. J. Biol. Macromol.*, DOI:10.1016/j.ijbiomac.2016.06.018.
45. S. B. Khan, F. Ali, T. Kamal, Y. Anwar, A. M. Asiri and J. Seo, *Int. J. Biol. Macromol.*, DOI:10.1016/j.ijbiomac.2016.03.026.
46. S. B. Khan, S. A. Khan, H. M. Marwani, E. M. Bakhsh, Y. Anwar, T. Kamal, A. M. Asiri and K. Akhtar, *RSC Adv.*, DOI:10.1039/c6ra21626a.
47. M. Ul-Islam, M. W. Ullah, S. Khan, T. Kamal, S. Ul-Islam, N. Shah and J. K. Park, *Recent Pat. Nanotechnol.*, 2016, **10**, 169-180.
48. X. Ji, Y. Xu, W. Zhang, L. Cui and J. Liu, *Compos. Part A Appl. Sci. Manuf.*, 2016, **87**, 29-45.
49. A. G. Xie, X. Cai, M. S. Lin, T. Wu, X. J. Zhang, Z. D. Lin and S. Tan, *Mater. Sci. Eng. B Solid-State Mater. Adv. Technol.*, DOI:10.1016/j.mseb.2011.06.020.
50. H. Hu, H. Liu, D. Zhang, J. Wang, G. Qin and X. Zhang, *Eng. Sci.*, 2018, 43–48.
51. J. Chen, H. Peng, X. Wang, F. Shao, Z. Yuan and H. Han, *Nanoscale*, , DOI:10.1039/c3nr04941h.
52. I. Armentano, M. Dottori, E. Fortunati, S. Mattioli and J. M. Kenny, in *Polymer Degradation and Stability*, 2010, **95**, 2126-2146.
53. N. Shah, T. Rehan and J. K. Park, *Polish J. Chem. Technol.*, DOI:10.1515/pjct-2016-0044.
54. A. V. Korobeinyk, R. L. D. Whitby and S. V. Mikhalovsky, *Eur. Polym. J.*,DOI:10.1016/j.eurpolymj.2011.10.006.
55. D. Shan, G. Cheng, D. Zhu, H. Xue, S. Cosnier and S. Ding, *Sensors Actuators, B Chem.*, , DOI:10.1016/j.snb.2008.11.029.

56. E. Y. Choi, T. H. Han, J. Hong, J. E. Kim, S. H. Lee, H. W. Kim and S. O. Kim, *J. Mater. Chem.*, , DOI:10.1039/b919074k.
57. Y. Yin, B. Jiang, X. Zhu, L. Meng and Y. Huang, *Eng. Sci.*, 2018, 17–19.
58. S. Lee, J. Kim, B.-C. Ku, J. Kim and H. I. Joh, *Adv. Chem. Eng. Sci.*, , DOI:10.4236/aces.2012.22032.
59. M. Naebe, J. Wang, A. Amini, H. Khayyam, N. Hameed, L. H. Li, Y. Chen and B. Fox, *Sci. Rep.*, DOI:10.1038/srep04375.
60. R. B. Mathur, O. P. Bahl, J. Mittal and K. C. Nagpal, *Carbon N. Y.*, 1991, **29**, 1059-1061.
61. K. Pal, A. K. Banthia and D. K. Majumdar, *AAPS PharmSciTech*, 2007, **8**, 142-146.
62. S. Kiatkamjornwong and J. Faullimmel, *J. Natl. Res. Counc. Thail.*
63. G. R. Mahdavinia, A. Pourjavadi, H. Hosseinzadeh and M. J. Zohuriaan, *Eur. Polym. J.*, DOI:10.1016/j.eurpolymj.2004.01.039.
64. N. Seddiki and D. Aliouche, *Bull. Chem. Soc. Ethiop.*, DOI:10.4314/bcse.v27i3.14.
65. S. Liu, T. H. Zeng, M. Hofmann, E. Burcombe, J. Wei, R. Jiang, J. Kong and Y. Chen, *ACS Nano*, DOI:10.1021/nn202451x.